

## Supplementary Materials

### Large transverse magneto-thermoelectric effect in narrow-band-gap polycrystalline $\text{Ag}_{2-\delta}\text{Te}$ †

Mingyu Chen,<sup>‡ab</sup> Tao Feng,<sup>‡c</sup> Nan Yin,<sup>d</sup> Quan Shi,<sup>d</sup> Peng Jiang<sup>\*ad</sup> and Xinhe Bao<sup>\*ad</sup>

<sup>a</sup>*State Key Laboratory of Catalysis, CAS Center for Excellence in Nanoscience, Dalian Institute of Chemical Physics, Chinese Academy of Sciences, Dalian 116023, Liaoning, China. E-mail: pengjiang@dicp.ac.cn, xhbao@dicp.ac.cn*

<sup>b</sup>*University of Chinese Academy of Sciences, Beijing 100049, China*

<sup>c</sup>*Department of Materials Science and Engineering, Southern University of Science and Technology, Shenzhen 518055, Guangdong, China*

<sup>d</sup>*Dalian National Laboratory for Clean Energy, Dalian Institute of Chemical Physics, Chinese Academy of Sciences, Dalian 116023, Liaoning, China*

†These authors contributed equally to the work.

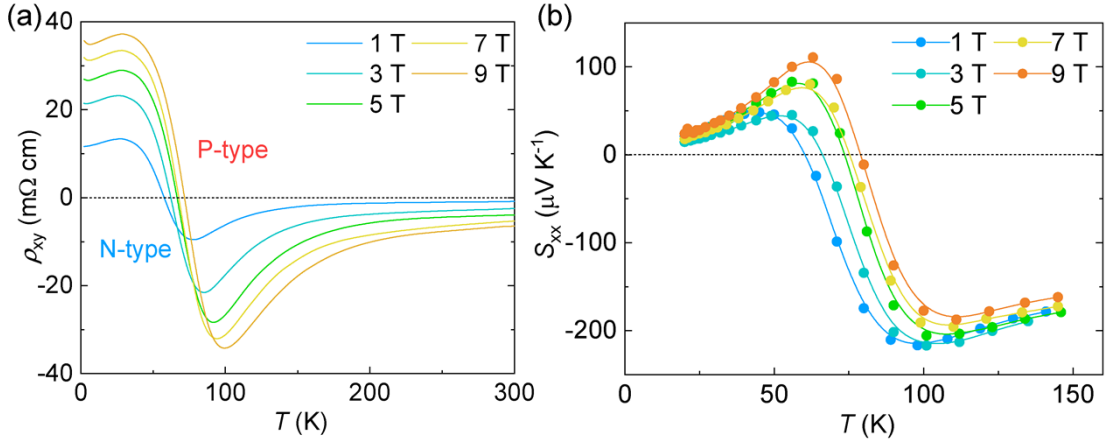


**Fig. S1** The temperature dependent (a) Hall resistivity  $\rho_{xy}$  and (b) Seebeck coefficient  $S_{xx}$  of  $\text{Ag}_{2-\delta}\text{Te}$  under the magnetic field of 1, 3, 5, 7, and 9 T. The N-P transition point shifts towards higher temperatures with the increase of the magnetic field.

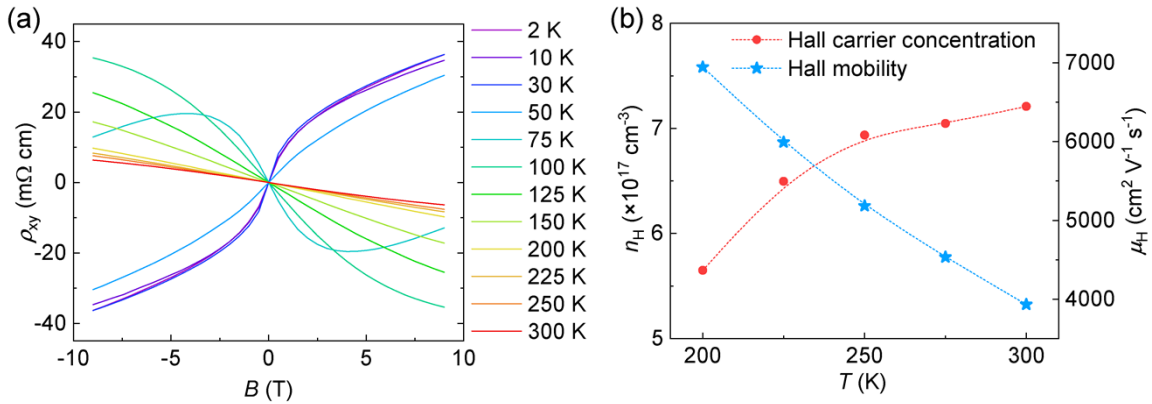


**Fig. S2** (a) The magnetic-field dependent Hall resistivity  $\rho_{xy}$  of  $\text{Ag}_{2-\delta}\text{Te}$  at various temperatures between 2 K and 300 K. (b) The Hall carrier concentration  $n_H$  and Hall mobility  $\mu_H$  of  $\text{Ag}_{2-\delta}\text{Te}$  at 200–300 K calculated based on the almost linear curve of  $\rho_{xy}$  in (a). The linear curves in (a) indicate that the sample is predominantly in a single-carrier model.

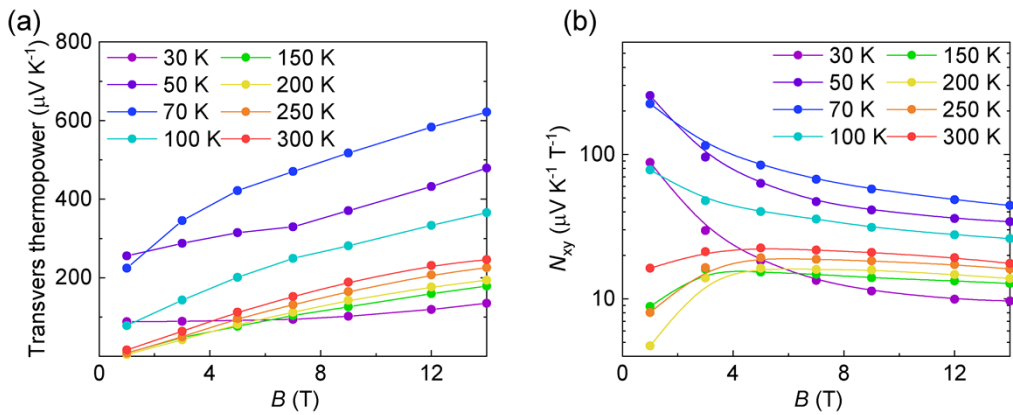


**Fig. S3** The magnetic-field-dependent transverse thermopower (a) and Nernst coefficient  $N_{xy}$  (b) of  $\text{Ag}_{2-\delta}\text{Te}$  under 1-14 T between 30 K and 300 K. The  $N_{xy}$  values are calculated by the magnetic-field-dependent transverse thermopower using  $N_{xy} = S_{xy}/\mu_0 H$ . The different behaviors on both sides of 100 K reveal the temperature-dependent band structure of  $\text{Ag}_{2-\delta}\text{Te}$ . It gradually deviates from a linear band structure as the temperature increases.

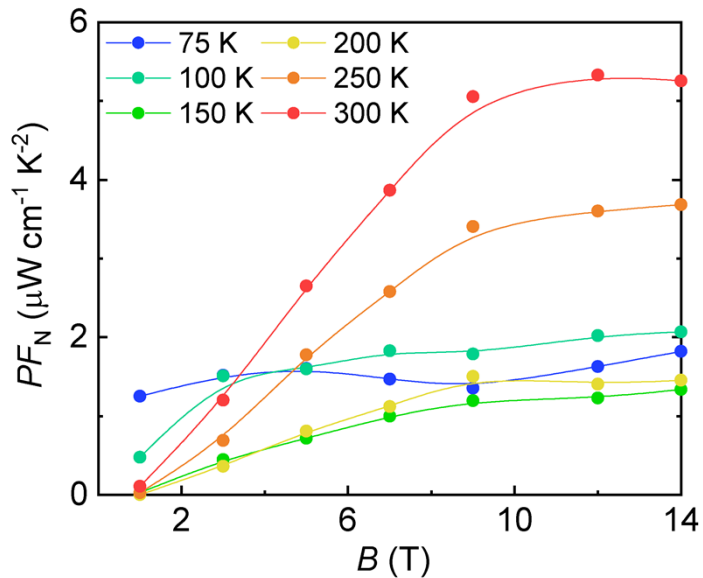


**Fig. S4** The magnetic-field-dependent transverse power factors  $PF_N$  of  $\text{Ag}_{2-\delta}\text{Te}$  under 1-14 T at various temperatures between 75 and 300 K. It saturates at 3 T below 100 K. As the temperature increases above 100 K, the saturated magnetic field reaches about 7 T.

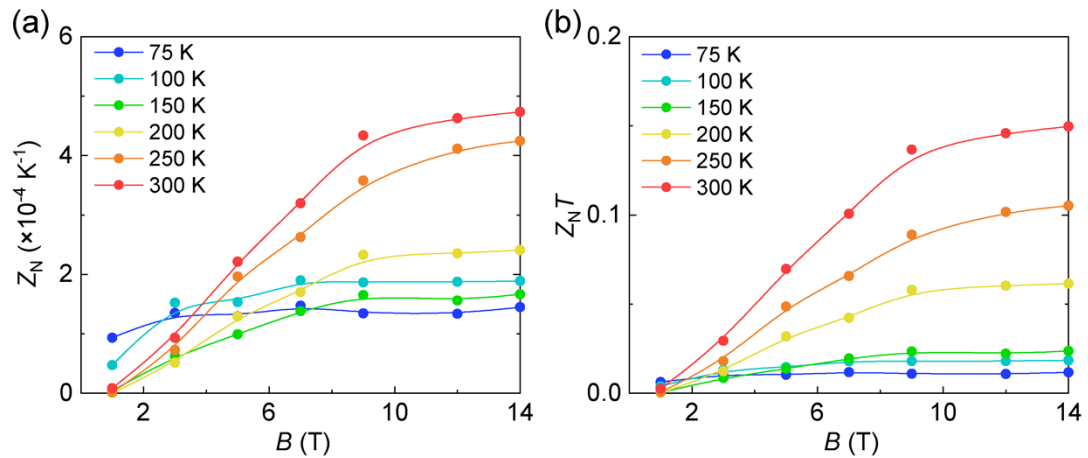


**Fig. S5** Magnetic field dependence of figure of merit  $Z_N$  (a) and  $Z_NT$  (b) in  $\text{Ag}_{2-\delta}\text{Te}$  under 1-14 T between 75 and 300 K. Both  $Z_N$  and  $Z_NT$  exhibit an initial increase followed by saturation as the magnetic field increases.

**Table S1** The average  $Z_N$  and the corresponding temperature range comparison of partial single-crystal and polycrystalline materials.

	Materials	Temperature range (K)	$\Delta T$ (K)	Average $Z_N$ ( $\times 10^{-4}$ K $^{-1}$ )
Single-crystal	WTe <sub>2</sub> <sup>1</sup>	7-16	9	193.8
	NbSb <sub>2</sub> <sup>2</sup>	5-70	65	26.6
	PtSn <sub>4</sub> <sup>3</sup>	5-30	25	9.4
	Bi <sub>97</sub> Sb <sub>3</sub> <sup>4</sup>	75-300	215	27.6
	Cd <sub>3</sub> As <sub>2</sub> <sup>5</sup>	100-350	250	12.1
	ZrTe <sub>5</sub> <sup>6</sup>	80-200	120	5.1
Polycrystalline	Ag <sub>2</sub> Se <sup>7</sup>	80-300	220	0.23
	NbP <sup>8</sup>	15-300	285	0.52
	NbP <sup>9</sup>	30-300	270	0.58
	Bi <sub>77</sub> Sb <sub>23</sub> <sup>10</sup>	50-300	250	2.15
	Ag <sub>2-δ</sub> Te (our work)	80-300	220	2.90
	NbSb <sub>2</sub> <sup>11</sup>	5-100	95	9.75

## References

- 1 Y. Pan, B. He, T. Helm, D. Chen, W. Schnelle and C. Felser, *Nat. Commun.*, 2022, **13**, 3909.
- 2 P. Li, P. F. Qiu, Q. Xu, J. Luo, Y. F. Xiong, J. Xiao, N. Aryal, Q. Li, L. D. Chen and X. Shi, *Nat. Commun.*, 2022, **13**, 7612.
- 3 C. G. Fu, S. N. Guin, T. Scaffidi, Y. Sun, R. Saha, S. J. Watzman, A. K. Srivastava, G. W. Li, W. Schnelle, S. S. P. Parkin, C. Felser and J. Gooth, *Research*, 2020, **2020**, 4643507.
- 4 K. F. Cuff, R. B. Horst, J. L. Weaver, S. R. Hawkins, C. F. Kooi and G. M. Enslow, *Appl. Phys. Lett.*, 1963, **2**, 145-146.
- 5 J. S. Xiang, S. L. Hu, M. Lyu, W. L. Zhu, C. Y. Ma, Z. Y. Chen, F. Steglich, G. F. Chen and P. J. Sun, *Sci. China Phys. Mech.*, 2020, **63**, 237011.
- 6 P. P. Wang, C. W. Cho, F. D. Tang, P. Wang, W. J. Zhang, M. Q. He, G. D. Gu, X. S. Wu, Y. H. Shao and L. Y. Zhang, *Phys. Rev. B*, 2021, **103**, 045203.
- 7 Y. Z. Lei, W. Liu, X. Y. Zhou, J. F. Luo, C. Zhang, X. L. Su, G. J. Tan, Y. G. Yan and X. F. Tang, *J. Solid State Chem.*, 2020, **288**, 121453.
- 8 C. G. Fu, S. N. Guin, S. J. Watzman, G. W. Li, E. K. Liu, N. Kumar, V. Suss, W. Schnelle, G. Auffermann, C. Shekhar, Y. Sun, J. Gooth and C. Felser, *Energy Environ. Sci.*, 2018, **11**, 2813-2820.
- 9 E. F. Scott, K. A. Schlaak, P. Chakraborty, C. G. Fu, S. N. Guin, S. Khodabakhsh, A. E. P. Y. Puente, C. Felser, B. Skinner and S. J. Watzman, *Phys. Rev. B*, 2023, **107**, 115108.
- 10 M. Murata, K. Nagase, K. Aoyama and A. Yamamoto, *Appl. Phys. Lett.*, 2020, **117**, 103903.
- 11 P. Li, P. F. Qiu, J. Xiao, T. T. Deng, L. D. Chen and X. Shi, *Energy Environ. Sci.*, 2023, **16**, 3753-3759.